Measurement: Sensors 18 (2021) 100215

Contents lists available at ScienceDirect

Measurement: Sensors

journal homepage: www.sciencedirect.com/journal/measurement-sensors

Characterization of high-power white leds for VLC applications

ARTICLE INFO

Keywords
Visible light communications
Light emitting diode
Impedance analyzer
Lock-in amplifier

ABSTRACT

During the last years, visible light communications (VLC) have been proposed for providing connectivity while ensuring satisfactory illumination in both indoor environments and also specific outdoor scenarios without the need of deploying complex infrastructures for that purpose. Transmission for VLC is carried out through light-emitting diodes (LEDs), which correspond to semiconductors based on PN-junction materials with a direct gap. In this sense, the current flow plays a major role in the behavior and performance of these devices for VLC. Therefore, characterizing the electrical response of high-power white LED results mandatory for the successful implementation of VLC. At this point, it is worth noting that the electrical characterization is usually not available for high-power LEDs since, in fact, determining these characterization results challenging. In this sense, there exist some measurement instruments such as LCRs or impedance analyzers typically employed for characterizing materials and passive electrical components. However, these kinds of instruments are subject to a limited input impedance and a maximum value of forwarding current. In this work, the electrical characterization of the LED LXHL-BW02 of Luxeon is analyzed to show that typically commercial instrumentation for characterizing these devices is limited for high-power LEDs, which may provide polluted results when these limitations are not considered. After that, the characterization of the LXHL-BW02 based on a lock-in amplifier is proposed.

1. Introduction

The first commercial LED corresponding to a red color was released in 1962. It consisted of a semiconductor light source based on the junction of PN materials with a direct gap. This configuration results in an efficient conversion of the electric current flow into light because of the spontaneous emission effect [1]. During the 70s, other colors were obtained varying the proportionality of the semiconductor materials to generate different emission wavelengths. In such a way, LEDs emitting a vast color palette, e.g., green, yellow, blue, etc. were developed [2,3]. In the 80s, the brightness of the LED was improved up to 10 times in comparison with the previous LEDs. This improvement was employed in new applications such as the advertisement displays that we see every day on the roads. From the 90s, the use of aluminum-galium-indium phosphorus allows us to generate a wide color palette from red to yellow by modifying the proportion of these materials while achieving a time of life greater than 100.000 hours [4].

Following this approach, in the middle of the 90s, high-efficiency blue LEDs appear to develop the first white light LED luminaires [5]. In this sense, there exist two methodologies for achieving white light. The first one is based on combining distinct red, green and blue (RGB) LEDs so that the resulting color corresponds to the mixture of these elementary colors. Notice that this approach does not generate only white light but any color with different tonalities. The other methodology for providing white light is based on adding a thin layer of phosphorus over a blue LED. Thus, the blue light stimulates the phosphorus layer until it starts to radiate yellow light because of the fluorescence of the phosphorus. The resulting combination of yellow light and blue light that is not absorbed by the phosphorus layer is detected by the human eye as white light [6]. Following this approach, the first commercial LED was released in 2002 providing a luminous efficiency of about 18–22 lm/W. In 2206, Narukawa et al. presented white LEDs composed of gallium-indium nitride achieving an efficiency of up to 174 lm/W subjects to a low current of about 2 mA. This LED architecture and the achieved efficiency can be considered a milestone to replace the conventional light bulbs for novel LED luminaires [7].

Nowadays, the illumination issues have been mostly solved and the research efforts are focused on providing optical communications by modulating the optical power to achieve data transmission in both indoor and outdoor scenarios while providing satisfactory illumination. This approach is typically referred to as visible light communications (VLC). The LED is polarized with a positive and constant voltage adding a modulated signal, typically with a small amplitude over this constant value. In this context, most of the works are focused on achieving high data rates by using similar modulations as RF systems such as WiFi or the fourth and five generations of cellular communications, i.e., 4G and 5G. However, in contrast to the aforementioned RF systems, VLC is still in a development phase, in which several challenges must be faced up yet [8].

In this work, we focus on one of these challenges, analyzing the electrical characterization of high-current LEDs. In this sense, the characterization of any LED can be represented as the proper combination of electronic passive components related to the physical response of the LED. Determining the correct value of these components involves measuring complex impedances. First, we describe the traditional characterization tools such as the impedance analyzer highlighting the

https://doi.org/10.1016/j.measen.2021.100215

Available online 27 September 2021

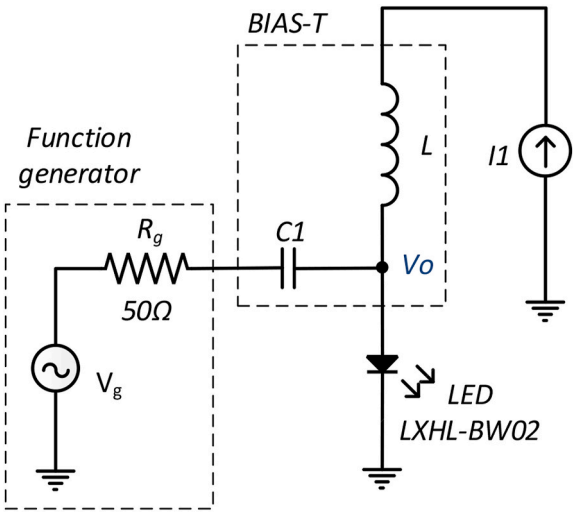

Fig. 1. Circuit for the impedance measurement of the diode.

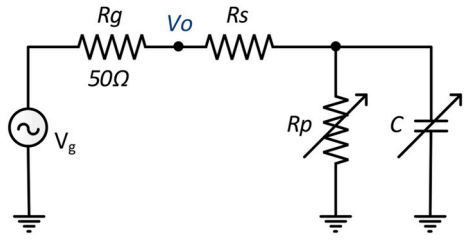

Fig. 2. Equivalent circuit in AC.

limitations that they are subject to. After that, we propose an alternative characterization procedure based on using a lock-in amplifier. Finally, a comparison between simulation and experimental results is presented to validate the proposed method.

2. Dynamic characterization of white leds

The PN junction comprises two approaches for managing the electric charge that has a direct impact on the response of the LED at high frequencies. These approaches correspond to using non-linear capacitances, usually referred to as barrier or depletion capacitance, and diffusion capacitance. These capacitances are denoted as C_f and C_{diff} from now on. The barrier capacitance is related to the charge given by the atom's ions between donors and acceptors. Notice that the extreme voltage modifies the charge at the junction area. Therefore, the barrier capacitance can be modeled as a flat capacitor. The diffusion capacitance is related to the exceed of charge injected by the minority carriers in direct polarization conditions. Both capacitances (barrier and diffusion) form a joint capacitance that has a direct impact on the temporal and frequency response of the diode. In parallel to these capacitances, the diode has a resistance that is sensitive to voltage variations (denoted as R_f) and a series resistance that models the neutral region between the PN junction (denoted as R_s).

To characterize the electrical response of the PN-junction diode, we propose the circuit depicted in Fig. 1. For this measurement methodology, the current source I1 sets the DC polarization and the capacitor C1 works as a coupling capacitance to add an AC signal over the polarization point.

The small-signal model of the diode can be reorganized as the circuit shown in Fig. 2. It is worth noticing that C is the sum of the barrier and diffusion capacitance.

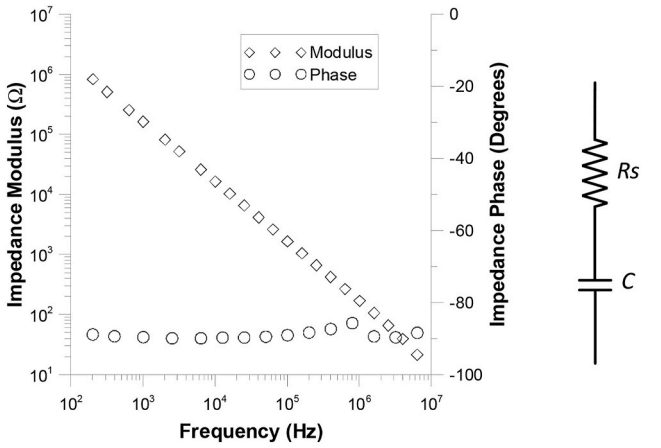

Fig. 3. Measurement of the complex impedance for DC bias range equal to 0 and equivalent electric circuit.

3. Impedance measurement using SOLARTRON 1260 analyzer

In this section, the measurement of the complex impedance, i.e., modulus and phase, of a white LED is performed using the SOLATRON 1260 analyzer, which provides a measurement bandwidth between 0.1 MHz and 32 MHz and a DC bias range equivalent to ±40.95 V and ±100mA for voltage and current modes, respectively. In the following, we focus on the LED LXHL-BW02 of LUXEON available in the diode library in the simulation software LTSPICE. This simulation software is employed further to validate the experimental results.

The first measurement is carried out considering a sinusoidal signal with a voltage equal to 10 mVRMS within a frequency range between 100 Hz and 5 MHz with a DC bias range of 0V. The modulus and phase of the measured impedance are shown in Fig. 3 following a Bode diagram. It can be seen that the diode is characterized by a capacitance performance, i.e., phase equal to 90°, corresponding to 0.95 nF, which is given by a barrier capacitor with a series resistance of 0.85 as also depicted in Fig. 4.

After that, a second measurement is carried out considering a DC bias range between 1 and 90 mA. The obtained results are shown in Fig. 4. At this point, it is worth remarking that for impedance values below 10 Ohm, the bandwidth range of the SOLARTRON 1260 analyzer is limited to 100 kHz, beyond this frequency the measured value can be misleading, usually obtaining peaks of impedance or values that do not make sense.

In Fig. 5, it can be seen that within the considered measurement bandwidth, below 100 kHz, the performance is purely resistive, i.e., phase equal to 0 because of the sum of the resistances R_s and R_p. It is worth noting that the value or the resistance R_p decreases as the polarization DC bias current increases.

Therefore, we can conclude that the value of the resistance R_p is constant and equal to a value given by a voltage of 83.57 mV divided by the polarization current IDC. Indeed, this constant is equal to $\eta \cdot K \cdot T/q$, where η is an experimental coefficient depending on the LED, K is the Boltzmann constant, T is the junction temperature and q is the electron charge.

4. Impedance measurement using a lock-in amplifier

As described in the previous section, the measurement process may be hampered by non-desired signals such as thermal noise whose voltage value can be similar to the desired signal. At this point, we focus on the use of lock-in amplifiers, which are typically proposed for measuring signals subject to noise. A lock-in amplifier consists of an analog multiplier followed by a low pass filter that turns the input signal at a specific frequency into a DC value or a very-low-frequency signal. To do

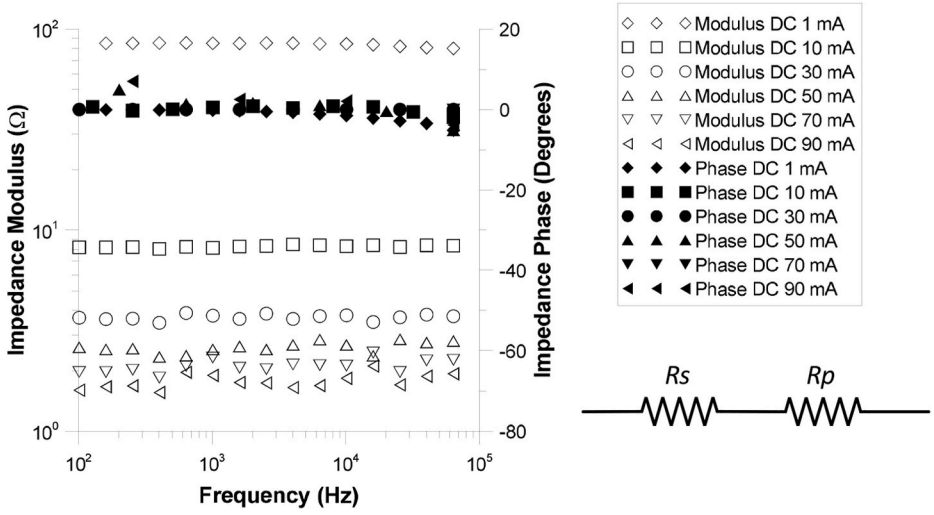

Fig. 4. Measurement of the complex impedance for DC bias range between 2 and 2,6 V.

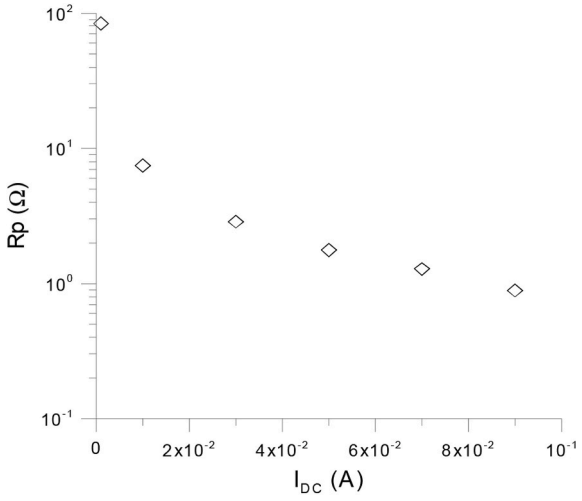

Fig. 5. Measurement of the resistance Rp.

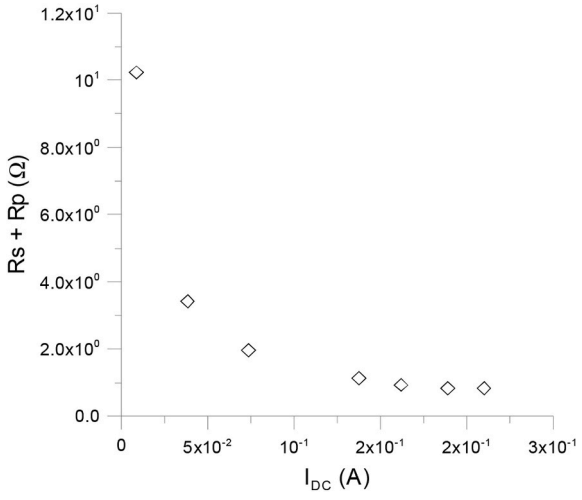

Fig. 6. Measurement of the impedance Rs + Rp.

so, it is required to implement a narrow bandpass filter to minimize the noise level while ensuring that the desired signal passes the filter. Therefore, both the measured signal and the bandpass filter must be determined by a reference signal, which must correspond to the same frequency as the signal desired to be measured.

In this work, the lock-in amplifier HF2LI of Zurich Instruments is considered because of its wide bandwidth, from DC to 50 MHz. The first step consists in calibrating the lock-amplifier by simply substituting de diode (see Figs. 1 and 2) by short value resistance, specifically, 1 Ω, 0.5 Ω and 0.25 Ω, which allow us to relate the output voltage of the lock amplifier with the value of the measured resistance.

The measured impedance of the considered LED LXHL-BW02 using the proposed methodology based on a lock amplifier is shown in Fig. 6. Specifically, a polarization current range between 8.6 mA and 210 mA is analyzed for measuring the impedance. As occurs in the methodology based on the SOLARTRON 1260 analyzer, the measured value of R_p decreases as the polarization current grows. For the current value above 160 mA, it can be seen in Fig. 6 that the value of R_s is about 0.83 Ω. Notice that this value is similar to the obtained by the impedance analyzer (see Fig. 5).

The effects of the capacitance C_2 are perceptible for frequencies above 1 MHz. The value of the impedance can be determined according to the following equations,

$$Z(\omega) = R_s + (R_p \parallel \frac{1}{j\omega c}) \tag{1}$$

$$C = \frac{\sqrt{R_p^2 - R_s^2 + (2 \cdot R_s \cdot Z(\omega))} - Z_r^2}{R_p \cdot \omega \sqrt{R_s^2 - (2 \cdot R_s \cdot Z(\omega)) + Z(\omega)^2}} \tag{2}$$

For measurement of the impedance at 10 MHz, the value of the capacitance is equal to 5.02 nF with a polarization current of 16 mA. In this sense, it has not been possible to obtain other measurements for higher polarization current as the intern capacitance of the lock-in amplifier interferes with the measurement. Although this capacitance depends on the polarization current, its contribution within the considered current range is relatively small. As a consequence, it is assumed that this capacitance remains constant within the employed current range.

5. Electric equivalent circuit for simulations

After a simple analysis of the circuit described in Figs. 2 and 3 is obtained,

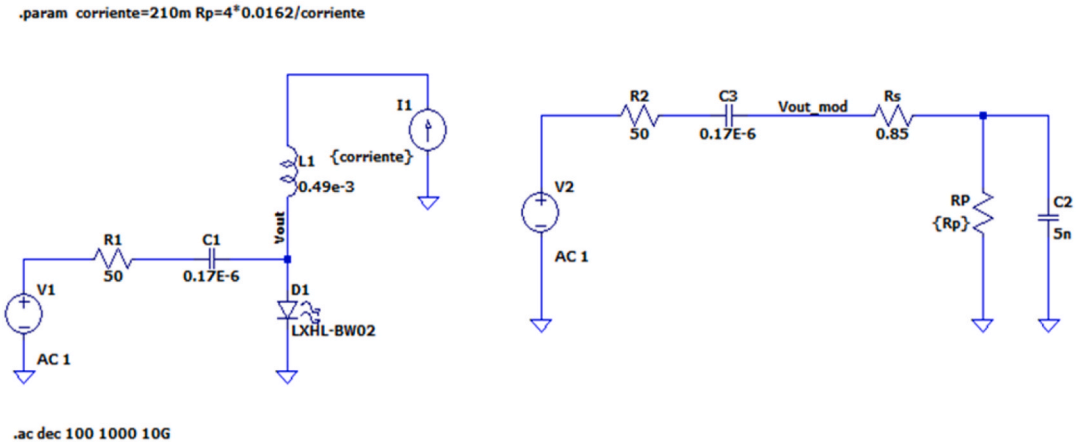

Fig. 7. Electrical circuit for simulation of the diode impedance.

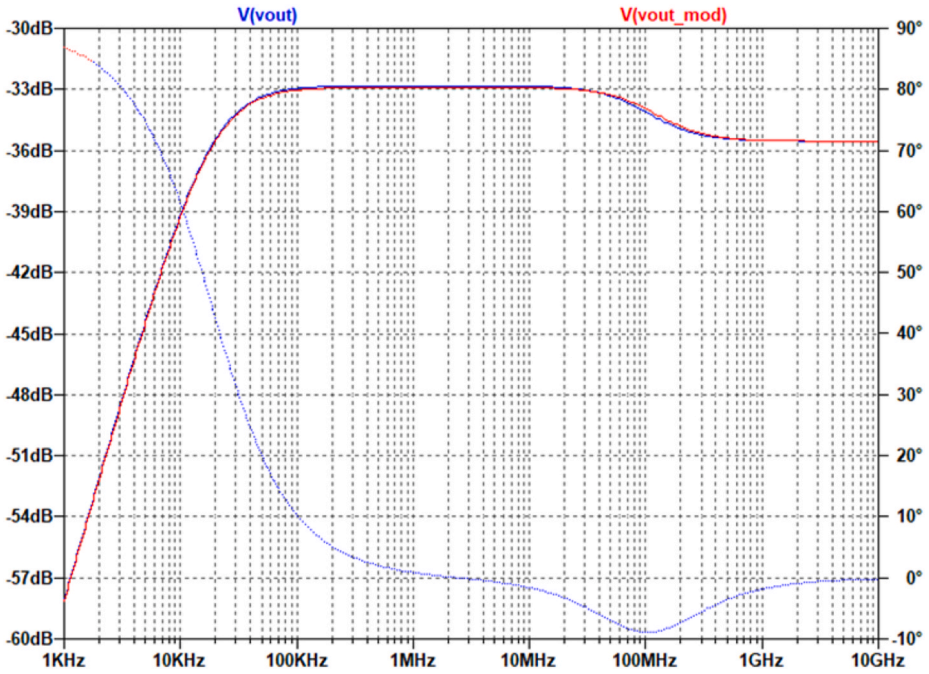

Fig. 8. Frequency response for the measurement circuit and the proposed approach for a polarization current of 210 mA.

$$\frac{V_0(s)}{V_i(s)} = G_0 \cdot \frac{1+\frac{s}{\omega_c}}{1+\frac{s}{\omega_p}}, \tag{3}$$

where,

$$G_0 = \frac{R_s + R_p}{R_g + R_s + R_p}, \tag{4}$$

$$\omega_c = \frac{R_s + R_p}{R_s \cdot R_p \cdot C_2}, \tag{5}$$

$$\omega_p = \frac{R_g + R_s + R_p}{R_p(R_g + R_s) \cdot C_2} \tag{6}$$

It can be easily seen that there are three main parameters: a constant G_0, a pole at ω_p, and a zero at ω_c. Then, can be concluded that the output resistance of the signal generator makes the zero to be close to the origin, while the pole is located at the right. Notice that, due to this pole the gain decreases until it stabilizes upon reaching the frequency corresponding to zero.

To validate the obtained results, the electric circuits depicted in Figs. 1 and 2 are simulated using the LTSPICE software. In this case, the model LXHL-BW02 available in the libraries of LTS-SPICE is considered in the simulations, comparing its behavior with the equivalent small-signal circuit obtained using the lock-in amplifier approach (see Fig. 7).

Then, a frequency sweep using LTSPICE is carried out for the voltage sources depicted in Fig. 7, from 1 kHz to 10 GHz. The obtained frequency response in modulus and phase of the voltage V_{out} and V_{out_mod} is shown in Fig. 8 and Fig. 9 for a polarization current equal to 210 mA and 16 mA, respectively.

It can be seen in these figures that the circuit contains a pole and a zero within the range of megahertz. In this sense, we can conclude that the proposed small-signal circuit provides a satisfactory and realistic performance of the diode model available in the libraries of the LTSPICE software.

6. Conclusions

The traditional impedance analyzers allow us to characterize materials and passive components. However, for high-power white LEDs,

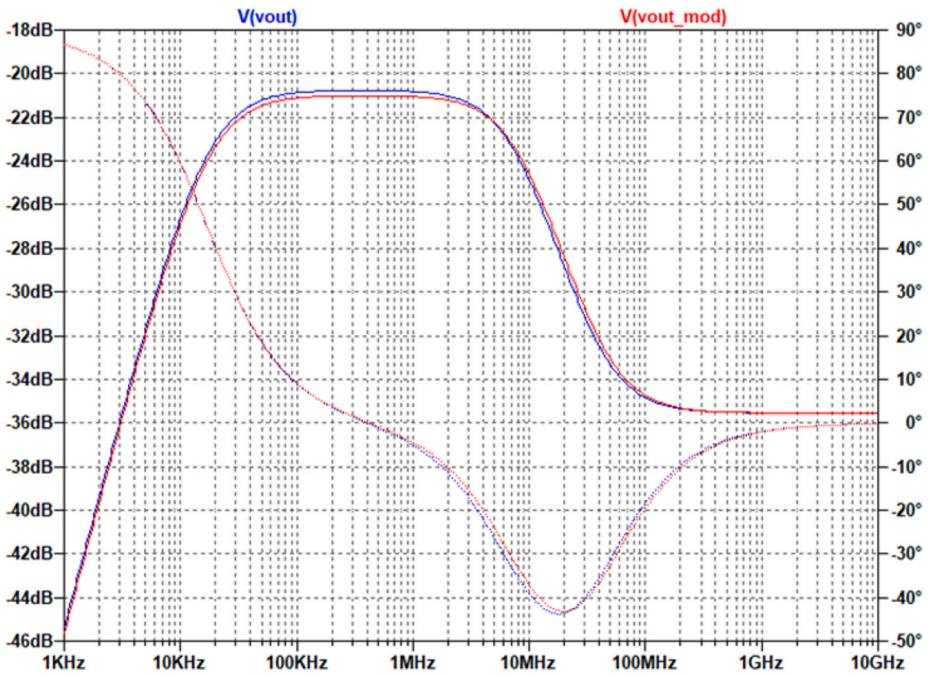

Fig. 9. Frequency response for the measurement circuit and the proposed approach for a polarization current of 16 mA.

specifically for the LED LXHL-BW02, due to its low resistance (below 10 Ω), the impedance analyzers are limited to low working frequencies (100 kHz range). At those frequencies (below 100 kHz) the LED has a pure resistance behavior. Therefore, the impedance analyzer results are useful for determining the values of the resistances R_s and R_p in the equivalent circuit of the LED. However, it is not possible to obtain knowledge about its dynamic performance.

In this work, we propose the use of a lock-in amplifier to characterize the capacitance elements of the LEDs for frequencies up to 50 MHz. On the other hand, the measurements are not focused on the characterization of the LED behavior due to changes in its polarization current. However, the simulation results show that increasing the polarization current carries a reduction of R_p, improving the electrical bandwidth of the equivalent circuit. Furthermore, it is worth remarking that the use of a bias tee device for polarizing the LED is not the most suitable approach since a large percentage of the signal from the generator falls into its output impedance.

Acknowledgments

This research was co-financed by Comunidad de Madrid and the FSE/FEDER Program under grant SINFOTON2-CM (S2018/NMT-4326), the Universidad Carlos III de Madrid under grant 2020/00038/001, and the Ministerio de Ciencia e Innovación and Agencia Estatal de Investigación (PID2019-109072RB-C31), and the European Regional Development Fund (ERDF) EXP 00119337/IDI-2019029.

References

[1] G.D. Clark, N. Holonyak, Optical properties of gallium arsenide-phosphide, Phys. Rev. 156 (3) (Apr. 1967) 913–924, https://doi.org/10.1103/PhysRev.156.913.
[2] M.G. Craford, Recent developments in light-emitting-diode technology, IEEE Trans. Electron. Dev. 24 (7) (Jul. 1977) 935–943, https://doi.org/10.1109/T-ED.1977.18854.
[3] T.P. Pearsall, B.I. Miller, R.J. Capik, K.J. Bachmann, 'Efficient lattice-matched double-heterostructure LED's at 1.1 μm from GaxIn1−xAsyP1−y', Appl. Phys. Lett. 28 (9) (May 1976) 499–501, https://doi.org/10.1063/1.88831.
[4] R.K. Willardson, E.R. Weber, G.B. Stringfellow, M.G. Craford, High Brightness Light Emitting Diodes, Elsevier Science, 1998.
[5] S. Nakamura, T. Mukai, M. Senoh, 'Candela-class high-brightness InGaN/AlGaN double-heterostructure blue-light-emitting diodes', Appl. Phys. Lett. 64 (13) (Mar. 1994) 1687–1689, https://doi.org/10.1063/1.111832.
[6] 'Visible Light Communications, Modulation and Signal Processing | Wiley', Wiley.com, 2017, in: https://www.wiley.com/en-us/Visible+Light+Communications%3A+Modulation+and+Signal+Processing-p-9781119331384. accessed Mar. 25, 2021.
[7] E. Balvís, R. Bendaña, H. Michinel, P.F. de Córdoba, A. Paredes, Analysis of a passive heat sink for temperature stabilization of high-power LED bulbs, J. Phys.: Conf. Ser. 605 (Apr. 2015), 012005, https://doi.org/10.1088/1742-6596/605/1/012005.
[8] S. Rajagopal, R.D. Roberts, S.-K. Lim, IEEE 802.15.7 visible light communication: modulation schemes and dimming support, IEEE Commun. Mag. (2012), https://doi.org/10.1109/MCOM.2012.6163585.

Juan S.Betancourt Perlaza*
Display and Photonic Applications Group, Electronic Technology Department, Carlos III University, Butarque 15, 28911, Leganés, Spain

Juan C. Torres
Display and Photonic Applications Group, Electronic Technology Department, Carlos III University, Butarque 15, 28911, Leganés, Spain
E-mail address: jctzafra@ing.uc3m.es.

Máximo Morales
Display and Photonic Applications Group, Electronic Technology Department, Carlos III University, Butarque 15, 28911, Leganés, Spain
E-mail address: mmcesped@ing.uc3m.es.

Iñaki Martínez-Sarriegui
Optiva Media, Edif. Europa II, Calle Musgo 2, 28023, Madrid, Spain
E-mail address: inaki.martinez@optivamedia.com.

Carlos I. del Valle
Optiva Media, Edif. Europa II, Calle Musgo 2, 28023, Madrid, Spain
E-mail address: carlosivan.delvalle@optivamedia.com.

José M. Sánchez Pena
Display and Photonic Applications Group, Electronic Technology Department, Carlos III University, Butarque 15, 28911, Leganés, Spain
E-mail address: jmpena@ing.uc3m.es.

* Corresponding author.
E-mail address: jbetanco@ing.uc3m.es (J.S.Betancourt Perlaza).